

# Quantitative Analysis of Excess Minority Carrier Density and Critical Duration in UV Irradiation-Based Screening for Bipolar Degradation in 4H-SiC

Yasuyuki Igarashi<sup>1,a\*</sup>, Kazumi Takano<sup>1,b</sup>, Yohsuke Matsushita<sup>1,c</sup>  
and Takuya Morita<sup>1,d</sup>

<sup>1</sup>ITES Co., Ltd., 1-60 Kuribayashi, Otsu, Shiga 520-2151, Japan

<sup>a</sup>yiga@ites.co.jp, <sup>b</sup>kazumi\_takano@ites.co.jp, <sup>c</sup>yohsuke\_matsushita@ites.co.jp,  
<sup>d</sup>takuya\_morita@ites.co.jp

**Keywords:** 4H-SiC, bipolar degradation, basal plane dislocation, stacking fault, UV screening, recombination-enhanced dislocation glide, minority-carrier lifetime.

**Abstract.** Ultraviolet (UV) irradiation on 4H-SiC epitaxial wafers, conducted prior to metallized circuit formation, is widely used to reveal whether BPD (basal plane dislocation) induced nucleation and expansion of a single Shockley stacking fault (1SSF) occurs via recombination enhanced dislocation glide (REDG). However, the UV method has remained largely qualitative, and its quantitative relationship to forward bias current injection has not been established. Here, using the excess minority carrier density at the BPD-to-TED (threading edge dislocation) conversion point, we establish equivalence criteria between two stress modes (current density and UV irradiance) and introduce a previously overlooked requirement for pulsed UV laser sources: the minority carrier density must exceed a threshold and be sustained for a finite “critical duration,”  $t_{crit}$ , defined as the minimum time required to initiate dislocation glide. Notably,  $t_{crit}$  shows only weak dependence on the bulk carrier lifetime ( $\tau_b$ ), offering a practical route to determine pulsed UV irradiation conditions that faithfully emulate forward bias stress, even when  $\tau_b$  is unknown.

## Introduction

Bipolar degradation, caused by the nucleation and expansion of 1SSF (single Shockley stacking fault) from BPD (basal plane dislocation) remains a key reliability concern for 4H-SiC bipolar power devices like PiN diodes and the body diode in MOSFETs. The conventional method for evaluating the impact of process modifications on bipolar degradation typically requires the fabrication of metallized active devices, followed by current injection testing. While highly reliable, this approach is costly and time intensive. As a simplified alternative, ultraviolet (UV) irradiation has been widely employed at the pre-circuit formation stage to verify the presence of defect expansion. UV irradiation is known to induce the nucleation and expansion of 1SSF from BPD through recombination enhanced dislocation glide (REDG) mechanism, similar to current injection. However, this method has been limited to qualitative assessments of 1SSF behavior and has not enabled quantitative equivalence, such as estimating the UV irradiation intensity corresponding to a specific current rating.

We have proposed a UV irradiation-based screening method (called E-V-C method) to detect latent BPD-related defects at an early stage by leveraging the SF expansion governed by REDG mechanism [1]. For practical deployment of the screening, however, it is essential to establish a quantitative equivalence between UV irradiation and forward bias current injection stress. We define UV irradiation conditions as equivalent to current injections if they allow identification of defect expansion with the same accuracy as current stress. Prior work [2], referencing Tawara et al. [3], reported that bar shaped 1SSF expansion occurs above a threshold current density, though device doping profiles influence the threshold value. Importantly, if we focus not on the current density but on the excess minority carrier density at the conversion point from BPD to TED (threading edge dislocation), where the stacking fault begins to expand, this density remains invariant to the device profile and is therefore defined as the critical minority carrier density. Based on this insight, we sought

to link the two stress modes, current injection and UV irradiation, via the critical minority carrier density generated under each condition.

A fundamental distinction, however, exists between the two stress modes. Constant current injection yields a steady state carrier distribution, whereas pulsed UV irradiation produces a transient carrier distribution that rises sharply post-pulse and decays exponentially. Therefore, in this study, we first independently determine, by experiment, the threshold conditions for SF expansion in each stress mode, namely, the threshold current density and the threshold UV irradiance. We then estimated the excess hole distributions using numerical calculations. By assuming equivalence of the hole density at the TED conversion point, we derived a correlation model. The analysis reveals that pulsed UV laser irradiation requires that the excess carrier density must not only exceed the threshold value for each pulse, but it must also persist above the value for a finite duration, herein termed “the critical duration”  $t_{crit}$ , a parameter absent under constant current injection case. This paper details the derivation of this equivalence condition for PiN diodes, incorporating the critical duration.

## Experiments and Results

PiN diodes were fabricated on commercial n-type 100 mm, 4H-SiC wafers (4 ° off-cut toward [11-20] direction). The structure comprised a buffer layer (0.5  $\mu\text{m}$ ,  $1 \times 10^{18} \text{ cm}^{-3}$ ) and a drift layer (5.4  $\mu\text{m}$ ,  $5 \times 10^{15} \text{ cm}^{-3}$ ), epitaxially grown on the substrate (350  $\mu\text{m}$ ,  $6 \times 10^{18} \text{ cm}^{-3}$ ). A 0.5  $\mu\text{m}$  p<sup>+</sup> anode layer was formed by Al doping ( $4.1 \times 10^{18} \text{ cm}^{-3}$ ). Ni electrode was deposited on the backside, and Al comb-shaped electrodes (2 mm square chips) were patterned on half the wafer for accelerated current stress tests; the remaining half was reserved for UV stress experiments.

Accelerated current stress tests were conducted with pulsed currents of 250–400 A/cm<sup>2</sup>. 1SSF expansion was monitored using UV photoluminescence (UVPL, 420 nm band pass filter), tracking Si(g) dislocation glide velocities. In parallel, UV irradiation was applied using a 355 nm Nd:YAG pulsed laser (10 ns pulse, 20  $\mu\text{s}$  period, duty 0.05 %, max 211  $\mu\text{J/pulse}$ , 3 mm beam). Output was varied from 1–100 % using an attenuator, and 1SSF expansion was studied at 10 %, 25 %, 50 %, and 100 % power.

Under current stress, 329 bar shaped 1SSF sites from 43 chips were analyzed (Fig. 1(a)), while 11 sites were examined under UV stress (Fig. 1(b)). Measured glide velocities varied significantly at identical stress levels, presumably attributed to numerous factors in real devices that can impede the motion of the Si(g) dislocation (e.g., various crystallographic defects). Because the goal of this study is to evaluate the correlation between stress intensity and expansion, linear regression was applied to the maximum-velocity data points at each stress level (red markers in Fig. 1(a), and (b)), where the influence of impeding factors is presumed to be minimal. Threshold intensities, defined as the zero-velocity intercepts, were determined as 235 A/cm<sup>2</sup> for current density and 36,650 W/cm<sup>2</sup> for UV irradiance, indicating equivalence between the two [2].

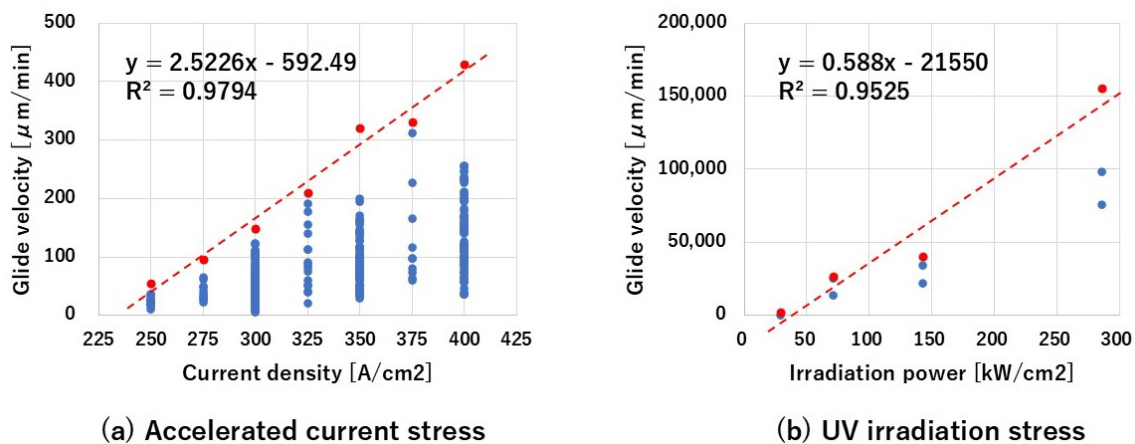


**Fig. 1.** Si(g) core glide velocity VS. stress intensity (current density (a) and irradiation power (b)).

## Numerical Analysis and Discussion

The experimentally determined threshold current density of  $235 \text{ A/cm}^2$  and UV irradiance of  $36,650 \text{ W/cm}^2$  were used to estimate hole densities, assuming equivalence at the critical minority carrier density. The device structure was  $p^+/n^-/n^+/n^{++}$  (anode, drift, buffer, substrate), with particular emphasis on the buffer layer, where BPD-to-TED conversion predominates.

The excess hole density  $\Delta p_{FB}(x)$  under forward bias was calculated by solving the carrier transport equation, assuming quasi-Fermi potential continuity at interfaces (i.e., a continuous  $pn$  product). The computed values near the  $n^-/n^{++}$  interface aligned reasonably with literature ( $1.8\text{--}2.5 \times 10^{16} \text{ cm}^{-3}$  [3]), though slightly lower as shown in Fig. 2. Since the hole density depends on the bulk minority carrier lifetime  $\tau_b$  in the  $n^-$  layer, which is unknown, the calculation was carried out by varying  $\tau_b$  from 50 ns to 2  $\mu\text{s}$ . The minority carrier lifetimes in the buffer layer and the substrate are also unknown; therefore, with reference to previous studies [4–6], they were assumed to be  $\tau_{\text{buffer}} = 30 \text{ ns}$  and  $\tau_{\text{sub}} = 3 \text{ ns}$ , respectively.

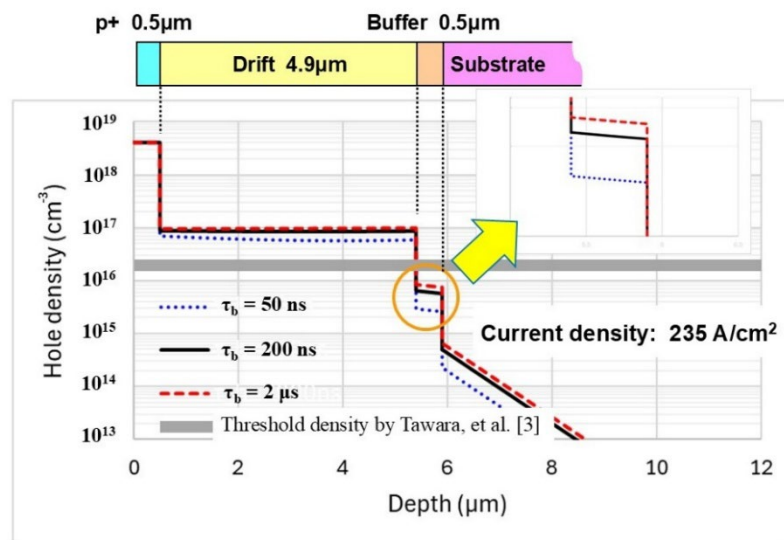


**Fig. 2.** Depth profiles of hole density under forward bias stress for the current density of  $235 \text{ A/cm}^2$ .

In contrast, under UV irradiation stress the hole density generated by the laser pulses becomes a function of both time and space. The excess hole density  $\Delta p_{UV}(x, t)$  was obtained from diffusion equations with Robin-type boundary conditions for surface recombination, continuity of carrier density and flux at layer interfaces, and an initial distribution set by Lambert-Beer's law for optical absorption immediately after UV exposure. Although a Fourier-series analytical solution is possible, a large number of higher-order terms are required for convergence; therefore a one-dimensional backward Euler finite difference method was employed to reduce computational load. Simulations were run for  $\tau_b = 50 \text{ ns}$ ,  $200 \text{ ns}$ , and  $2 \mu\text{s}$ , as shown in Fig. 3(a), (b), (c), respectively.  $\tau_{\text{buffer}}$  and  $\tau_{\text{sub}}$  were assumed to be the same as in forward bias case.

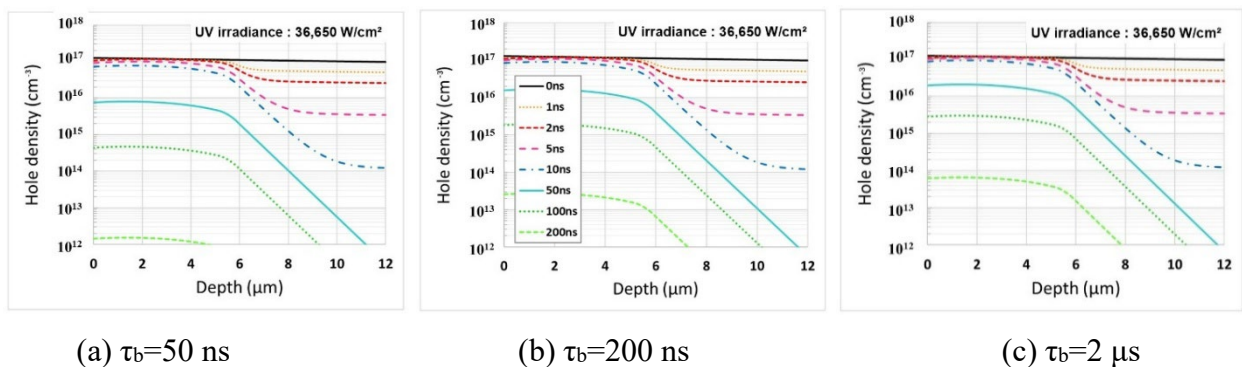


**Fig. 3.** Depth profiles of hole density under UV irradiation stress for  $\tau_b = 50 \text{ ns}$ ,  $200 \text{ ns}$ ,  $2 \mu\text{s}$  for the UV irradiance of  $36,650 \text{ W/cm}^2$ .

Since many BPD-to-TED conversion points are thought to distribute near the buffer/substrate and buffer/drift interfaces, the hole density at these locations was monitored over time. Figure 4 shows decay curves for  $\tau_b = 50$  ns and  $2 \mu\text{s}$ . Figure 5 overlays these curves with forward bias results (from Fig. 2). It is an enlarged view of Figure 4, highlighting the region that includes the point—within the range of  $\tau_b = 50$  ns to  $2 \mu\text{s}$ —at which the hole density under forward bias intersects with the decay curve of the hole density after UV pulse irradiation (i.e., the point where the two become identical). The vertical axis has been changed from a logarithmic scale to a linear scale.

Black triangles indicate the points where UV induced hole densities fall to the forward bias threshold level. This level can be interpreted as the minimum duration required for the initiation of 1SSF expansion. Specifically, it corresponds to the time needed for the leading edge of the Si(g) core dislocation to overcome the Peierls potential and initiate the local 4H to 3C transformation. This duration is defined as the critical time,  $t_{\text{crit}}$ . Notably,  $t_{\text{crit}}$  exhibits only a weak dependence on the bulk carrier lifetime in the drift layer,  $\tau_b$ . As shown in Figs. 2–4, the hole density in the buffer layer changes significantly with  $\tau_b$ , but the direction of this change is the same under both forward bias and UV irradiation conditions. Consequently,  $t_{\text{crit}}$  itself is expected to vary little. By contrast, although not discussed in detail here, an increase in the minority carrier lifetime in the buffer layer or the substrate results in a longer  $t_{\text{crit}}$ —defined as the decay time required for the hole density after UV irradiation to converge to that under forward bias current injection—whereas a decrease leads to a shorter  $t_{\text{crit}}$ .

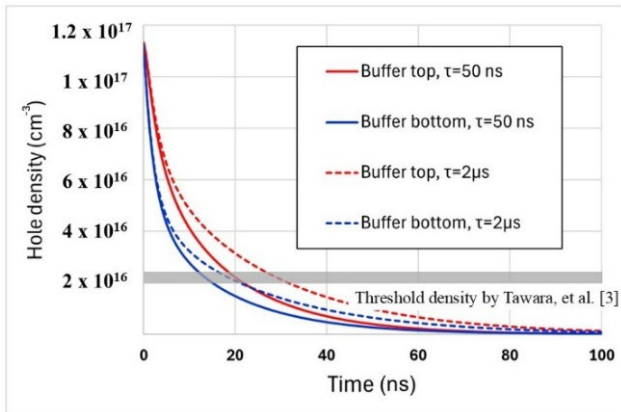


**Fig. 4.** Decay curves of hole density.

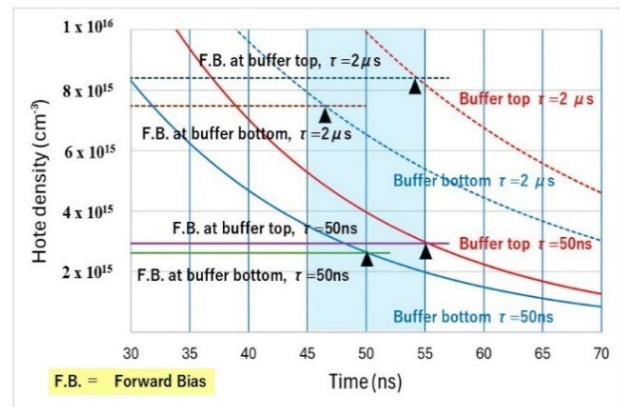


**Fig. 5.** The same hole density points ▲ (Superimposed on Fig. 4 with Fig. 2).

As shown in Fig. 6,  $t_{\text{crit}}$  remained approximately constant ( $\sim 50 \pm 5$  ns) across  $\tau_b = 50$  ns to  $2 \mu\text{s}$ , with negligible dependence on  $\tau_b$ . The same figure also shows (right y-axis) the  $\tau_b$  dependence of the hole density.

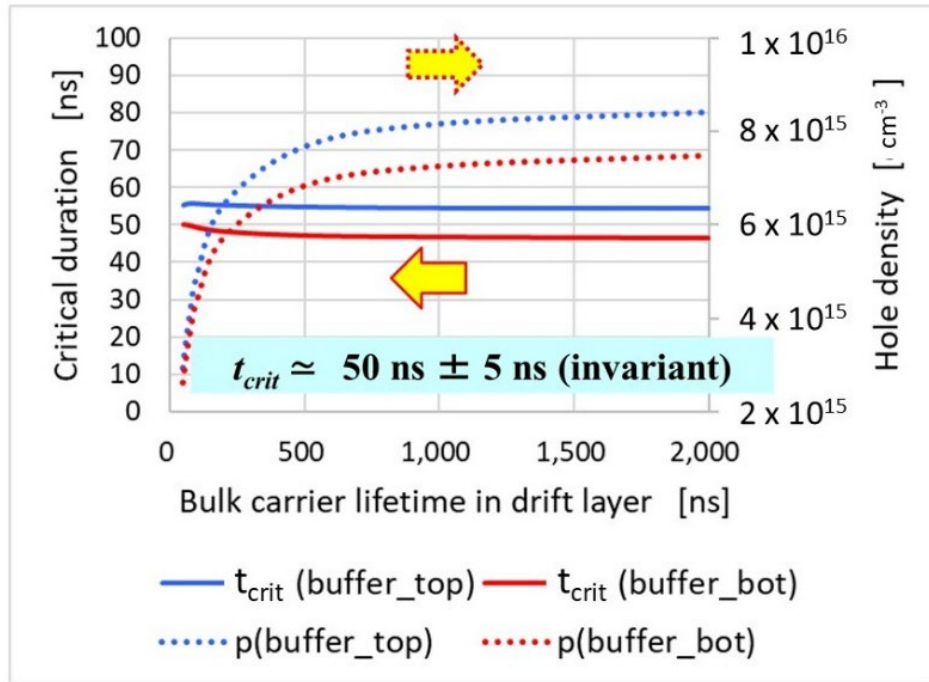


**Fig. 6.** Critical duration ( $t_{crit}$ ) over the range of carrier lifetime from 50 ns to 2  $\mu$ s.

Therefore, a UV condition equivalent to a given forward bias condition can be defined by the following equation (1). At a conversion point  $x_0$  in the buffer

$$\Delta p_{UV}(x_0, t_{crit}) = \Delta p_{FB}(x_0). \quad (1)$$

This provides a practical guideline for setting UV irradiation parameters for screening BPD-related defects. Moreover, the weak dependence of  $t_{crit}$  on carrier lifetime implies that even if  $\tau_b$  is unknown, its impact on the equivalency is limited.

## Summary

We demonstrated that 1SSF nucleation/expansion under pulsed UV irradiation requires not only exceeding the threshold hole density but also sustaining it for the critical time  $t_{crit}$ . This duration represents the minimum time to overcome the Peierls barrier associated with the 4H-to-3C transformation. Notably,  $t_{crit}$  is nearly independent of the bulk minority carrier lifetime  $\tau_b$  in the  $n^-$  layer. To replicate forward bias degradation via pulsed laser irradiation, conditions must yield hole densities matching those under forward bias, sustained for  $t_{crit}$  (Eq. (1)). The dependence of  $t_{crit}$  on the minority carrier lifetimes in the buffer layer and the substrate will be investigated in detail in future studies. While the equivalence estimation in this study relied on statistical analysis of multiple defects, future work will aim to directly validate Eq. (1) by examining the expansion behavior of identical defects. This will be pursued sequentially through UV stress, annealing-induced 1SSF contraction (300–600 °C), and subsequent current injection stress.

## Acknowledgment

This work was supported by the Ministry of Economy, Trade and Industry (METI) R&D Support Program for Growth-Oriented Technology SMEs (Grant No. JPJ005698). The authors gratefully acknowledge the technical guidance of Prof. Kato (Nagoya Institute of Technology) and Assoc. Prof. Harada (Nagoya University).

**References**

- [1] Y. Igarashi, K. Takano, Y. Matsushita, C. Shibata, Defect and Diffusion Forum, vol. 425, p. 75, 2023.
- [2] Y. Igarashi, K. Takano, Y. Matsushita, C. Shibata, Defect and Diffusion Forum, vol. 434, p. 23, 2024.
- [3] T. Tawara, S. Matsunaga, T. Fujimoto, M. Ryo, M. Miyazato, T. Miyazawa, K. Takenaka, M. Miyajima, A. Otsuki, Y. Yonezawa, T. Kato, H. Okumura, T. Kimoto, and H. Tsuchida, J. Appl. Phys., vol. 123, 025707, 2018.
- [4] T. Tawara, T. Miyazawa, M. Ryo, M. Miyazato, T. Fujimoto, K. Takenaka, S. Matsunaga, M. Miyajima, A. Otsuki, Y. Yonezawa, T. Kato, H. Okumura, T. Kimoto, H. Tsuchida, J. Appl. Phys. 120, 115101 (2016).
- [5] A. Y. Polyakov, Q. Li, S. Wook Huh, M. Skowronski, O. Lopatiuk, L. Chernyak, and E. Sanchez, J. Appl. Phys. 97, 053703 2005.
- [6] W. A. Doolittle, A. Rohatghi, R. Ahrienkel, D. Levi, G. Augustine, and R. H. Hopkins, Mater. Res. Soc. Symp. Proc. 483, 197 1998.